HAL open science

Computing Stieltjes constants using complex integration

Fredrik Johansson, Iaroslav V Blagouchine

▶ **To cite this version:**

Fredrik Johansson, Iaroslav V Blagouchine. Computing Stieltjes constants using complex integration. Mathematics of Computation, 2019, 88 (318), 10.1090/mcom/3401 . hal-01758620v3

HAL Id: hal-01758620

https://inria.hal.science/hal-01758620v3

Submitted on 11 Aug 2018

HAL is a multi-disciplinary open access archive for the deposit and dissemination of scientific research documents, whether they are published or not. The documents may come from teaching and research institutions in France or abroad, or from public or private research centers.

L'archive ouverte pluridisciplinaire **HAL**, est destinée au dépôt et à la diffusion de documents scientifiques de niveau recherche, publiés ou non, émanant des établissements d'enseignement et de recherche français ou étrangers, des laboratoires publics ou privés.

COMPUTING STIELTJES CONSTANTS USING COMPLEX INTEGRATION

FREDRIK JOHANSSON AND IAROSLAV V. BLAGOUCHINE

Abstract. The generalized Stieltjes constants $\gamma_n(v)$ are, up to a simple scaling factor, the Laurent series coefficients of the Hurwitz zeta function $\zeta(s,v)$ about its unique pole $s=1$. In this work, we devise an efficient algorithm to compute these constants to arbitrary precision with rigorous error bounds, for the first time achieving this with low complexity with respect to the order n. Our computations are based on an integral representation with a hyperbolic kernel that decays exponentially fast. The algorithm consists of locating an approximate steepest descent contour and then evaluating the integral numerically in ball arithmetic using the Petras algorithm with a Taylor expansion for bounds near the saddle point. An implementation is provided in the Arb library. We can, for example, compute $\gamma_n(1)$ to 1000 digits in a minute for any n up to $n=10^{100}$. We also provide other interesting integral representations for $\gamma_n(v)$, $\zeta(s)$, $\zeta(s,v)$, some polygamma functions and the Lerch transcendent.

1. Introduction

The Hurwitz zeta function $\zeta(s,v)=\sum_{k=0}^{\infty}(k+v)^{-s}$ is defined for all complex $v\neq 0,-1,-2,\dots$ and by analytic continuation for all complex s except for the point $s=1$, at which it has a simple pole. The Laurent series in a neighborhood of this unique pole is usually written as

$$\zeta(s,v)=\frac{1}{s-1}+\sum_{n=0}^{\infty}\frac{(-1)^n}{n!}\gamma_n(v)(s-1)^n\,,\qquad s\in\mathbb{C}\setminus\{1\}. \tag{1}$$

The coefficients $\gamma_n(v)$ are known as the generalized Stieltjes constants. The ordinary Stieltjes constants $\gamma_n=\gamma_n(1)$, appearing in the analogous expansion of the Riemann zeta function $\zeta(s)=\zeta(s,1)$, are also known as the generalized Euler constants and include the Euler-Mascheroni constant $\gamma_0=\gamma=0.5772156649\dots$ as a special case.[1]

This work presents an original method to compute $\gamma_n(v)$ rigorously to arbitrary precision, with the property of remaining fast for arbitrarily large n. Such an algorithm has never been published (even in the case of $v=1$), despite an extensive literature dedicated to the Stieltjes constants. At the heart of the method is Theorem 1, given below in Section 2, which provides computationally viable integral

Date: XXX and, in revised form, XXX.

2010 *Mathematics Subject Classification.* Primary 11M35, 65D20; Secondary 65G20.

Key words and phrases. Stieltjes constants, Hurwitz zeta function, Riemann zeta function, integral representation, complex integration, numerical integration, complexity, arbitrary-precision arithmetic, rigorous error bounds.

representations for $\zeta(s,v)$ and $\gamma_n(v)$. In particular, for $n \in \mathbb{N}_0$ and $\mathrm{Re}(v) > \frac{1}{2}$,

$$\gamma_n(v) = -\frac{\pi}{2(n+1)} \int_{-\infty}^{+\infty} \frac{\log^{n+1}(v - \frac{1}{2} + ix)}{\cosh^2 \pi x}\, dx, \tag{2}$$

which extends representation (5) from [5] to the generalized Stieltjes constants. The above expression is similar to the Hermite formula

$$\gamma_n(v) = \left(\frac{1}{2v} - \frac{\log v}{n+1}\right) \log^n v - i \int_0^{\infty} \frac{dx}{e^{2\pi x} - 1} \left\{ \frac{\log^n(v - ix)}{v - ix} - \frac{\log^n(v + ix)}{v + ix} \right\}, \tag{3}$$

see e.g. [5, Eq. 13], but more convenient to use for computations since the integrand with the hyperbolic kernel $\mathrm{sech}^2 \pi x$ does not possess a removable singularity at $x = 0$. Additionally, Section 2 provides some other integral representations for $\zeta(s,v)$ and $\gamma_n(v)$, some of which may also be suitable for computations (see, in particular, Corollary 1 and Remark 1).

Section 3 describes a robust numerical integration strategy for computing $\gamma_n(v)$. A crucial step is to determine an approximate steepest descent contour that avoids catastrophic oscillation for large n. This is combined with validated integration to ensure that the computation is accurate (indeed, yielding proven error bounds). An open source implementation is available in the Arb library [14]. Section 4 contains benchmark results.

1.1. **Background.** The numbers γ_n with $n \le 8$ were first computed to nine decimal places by Jensen in 1887. Many authors have followed up on this work using an array of techniques. Fundamentally, any method to compute $\zeta(s)$ or $\zeta(s,v)$ can be adapted to compute γ_n or $\gamma_n(v)$ respectively by taking derivatives. For example, as discussed by Gram [12], Liang and Todd [21], Jensen's calculations of γ_n were based on the limit representation

$$\zeta(s) = \lim_{N\to\infty} \left\{ \sum_{k=1}^{N} \frac{1}{k^s} - \frac{N^{1-s}}{1-s} \right\}, \qquad \mathrm{Re}(s) > 0\,, \tag{4}$$

which follows from the Euler–Maclaurin summation formula, so that

$$\gamma_n = \lim_{N\to\infty} \left\{ \sum_{k=1}^{N} \frac{\log^n k}{k} - \frac{\log^{n+1} N}{n+1} \right\}, \qquad n \in \mathbb{N}_0\,,$$

while Gram expressed γ_n in terms of derivatives of the Riemann ξ function which he evaluated using integer zeta values. Liang and Todd proposed computing γ_n either via the Euler-Maclaurin summation formula for $\zeta(s)$, or, as an alternative, via the application of Euler's series transformation to the alternating zeta function. Bohman and Fröberg [8] later refined the limit formula technique.

Formula (3) is a differentiated form of Hermite's integral representation for $\zeta(s,v)$, which can be interpreted as the Abel-Plana summation formula applied to the series for $\zeta(s,v)$. As discussed by Blagouchine [5], the formula (3) has been rediscovered several times in various forms (the $v = 1$ case should be credited to Jensen and Franel and dates back to the end of the XIXth century). Ainsworth and Howell [2] rediscovered the $v = 1$ case of (3) and were able to compute γ_n up to $n = 2000$ using Gaussian quadrature.

[1] Its generalized analog $\gamma_0(v)$ includes the digamma function $\Psi(v)$, namely $\gamma_0(v) = -\Psi(v)$, see e.g. [5, Eq. (14)].

Keiper [18] proposed an algorithm based on the approximate functional equation for computing the Riemann ξ function, which upon differentiation yields derivatives of $\xi(s)$ as integrals involving Jacobi theta functions. The Stieltjes constants are then recovered by a power series transformation.

Kreminski [20] used a version of the limit formula combined with Newton-Cotes quadrature to estimate the resulting sums, and computed accurate values of $\gamma_n(v)$ up to $n = 3200$ for $v = 1$ and up to $n = 600$ for various rational v. More recently, Johansson [13] combined the Euler-Maclaurin formula with fast power series arithmetic for computing $\gamma_n(v)$, proved rigorous error bounds for this method, and performed the most extensive computation of Stieltjes constants to date resulting in 10000-digit values of γ_n for all $n \leq 10^5$.

Even more recently, Adell and Lekuona [1] have used probability densities for binomial processes to obtain new rapidly convergent series for γ_n in terms of Bernoulli numbers.

The drawback of the previous methods is that the complexity to compute γ_n is at least linear in n. In most cases, the complexity is actually at least quadratic in n since the formulas tend to have a high degree of cancellation necessitating use of $\Omega(n)$-digit arithmetic. For the same reason, the space complexity is also usually quadratic in n, at least in the most efficient forms of the algorithms. For numerical integration of (3), the difficulty for large n lies in the oscillation of the integrand which leads to slow convergence and catastrophic cancellation.[2]

The fast Euler-Maclaurin method [13] does allow computing $\gamma_0, \ldots, \gamma_n$ simultaneously to a precision of p bits in $n^{2+o(1)}$ time if $p = \Theta(n)$, which is quasi-optimal. However, this is not ideal if we only need $p = O(1)$ or a single γ_n.[3]

This leads to the question of whether we can compute γ_n quickly for any n; ideally, in time depending only polynomially on $\log(n)$. If we assume that the accuracy goal p is fixed, then any asymptotic formula $\gamma_n \sim G(n)$ where $G(n)$ is an easily computed function should do the job.

Various asymptotic estimates and bounds for the Stieltjes constants have been published, going back at least to Briggs [10] and Berndt [3],[4] but the explicit computations by Kreminski and others showed that these estimates were far from precise.

A breakthrough came in 1984, when Matsuoka succeeded in obtaining the first–order asymptotics for the Stieltjes constants [23], [27, p. 3]. Four years later he derived the complete asymptotic expansion

$$\begin{aligned}\gamma_n \sim \frac{n!\, e^{g(b)}}{\pi} \sum_{k=0}^{N} \frac{|h_{2k}|\, 2^{k+\frac{1}{2}}\, \Gamma(k+\frac{1}{2})}{\left(g''(b)^2 + f''(b)^2\right)^{\frac{1}{2}k+\frac{1}{4}}} \times \\ \times \cos\left[f(b) - (k+\tfrac{1}{2}) \arctan \frac{f''(b)}{g''(b)} + \arctan \frac{v_{2k}}{u_{2k}}\right], \quad N = 0, 1, 2, \ldots\end{aligned} \tag{5}$$

[2]The formula (3) has also been used by Johansson for a numerical implementation of Stieltjes constants in the mpmath library [16], but the algorithm as implemented in mpmath loses accuracy for large n (for example, $\gamma_{10^4} \approx -2.21 \cdot 10^{6883}$ but mpmath 1.0 computes $-1.25 \cdot 10^{6800}$).

[3]It is of course also interesting to consider the complexity of computing a single γ_n value to variable accuracy p. For $n \geq 1$, the complexity is $\Omega(p^2)$ with all known methods (although the fast Euler-Maclaurin method amortizes this to $p^{1+o(1)}$ per coefficient when computing $n = \Theta(p)$ values simultaneously). The exception is γ_0 which can be computed in time $p^{1+o(1)}$ by exploiting its role as a hypergeometric connection constant [9].

[4]For the more complete history, see [6, Sect. 3.4].

where h_k, v_k and u_k are the sequences of numbers defined by

$$\sum_{k=0}^{\infty} h_k (y-b)^k \;=\; \exp\Big[\phi(a+iy) - \phi(a+ib) + \tfrac{1}{2}\phi''(a+ib)(y-b)^2\Big]\,,$$

$$u_k \equiv \mathrm{Re}(h_k)\,, \qquad v_k \equiv \mathrm{Im}(h_k)\,,$$

and $f(b)$ and $g(b)$ are the functions defined as

$$g(y) \equiv \mathrm{Re}\,\phi(a+iy)\,, \qquad f(y) \equiv \mathrm{Im}\,\phi(a+iy)\,,$$

$$\phi(z) \;=\; -(n+1)\log z - z\log 2\pi i + \log\Gamma(z)\,.$$

The pair $a = \mathrm{Re}\,z$, $b = \mathrm{Im}\,z$, is the unique solution of the equation

$$\frac{d\phi(z)}{dz} \;=\; -\frac{n+1}{z} - \log 2\pi i + \Psi(z) \;=\; 0\,, \tag{6}$$

satisfying $0 < \mathrm{Im}\,z < \mathrm{Re}\,z$ and $\sqrt{n} < \mathrm{Re}\,z < n$, where $\Gamma(z)$ and $\Psi(z)$ are the gamma and digamma functions respectively, see [24, pp. 49–50].[5] The Matsuoka expansion (5) accurately predicts the behavior of γ_n, but is very cumbersome to use. In 2011 Knessl and Coffey [19] presented a simpler asymptotic formula[6]

$$\gamma_n \sim \frac{B}{\sqrt{n}} e^{nA} \cos(an+b) \tag{7}$$

in terms of the slowly varying functions

$$A = \frac{1}{2}\log(\alpha^2+\beta^2) - \frac{\alpha}{\alpha^2+\beta^2}, \quad B = \frac{2\sqrt{2\pi(\alpha^2+\beta^2)}}{\sqrt[4]{(\alpha+1)^2+\beta^2}},$$

$$a = \arctan\frac{\beta}{\alpha} + \frac{\beta}{\alpha^2+\beta^2}, \quad b = \arctan\frac{\beta}{\alpha} - \frac{1}{2}\arctan\frac{\beta}{\alpha+1},$$

where β is the unique solution of

$$2\pi\exp(\beta\tan\beta) = \frac{n\cos\beta}{\beta}\,, \qquad \text{with} \quad 0 < \beta < \tfrac{1}{2}\pi, \quad \alpha = \beta\tan\beta\,.$$

In (7), the "$\sim$" symbol signifies asymptotic equality as long as the cosine factor is bounded away from zero. The factor $Be^{nA}/\sqrt{n}$ captures the overall growth rate of γ_n while the cosine factor explains the local oscillations (and semi-regular sign changes).

More recently, Fekih-Ahmed [11] has given an alternative asymptotic formula with similar accuracy to (7). Paris [25] has also generalized (7) to $\gamma_n(v)$ and extended the result to an asymptotic series with higher order correction terms, permitting the determination of several digits for moderately large n.

The Matsuoka, Knessl-Coffey, Fekih-Ahmed and Paris formulas were obtained using the standard asymptotic technique of applying saddle point analysis to a suitable contour integral. From a computational point of view, these formulas still have three drawbacks. First, being asymptotic in nature, they only provide a fixed level of accuracy for a fixed n, so a different method must be used for small n and high precision p. Second, the terms in Matsuoka's expansion and the high-order

[5] Matsuoka's Lemma 1 may be written in our form (6) if we notice that equations (2) and (3) [24, p. 49] actually represent one single equation in which real and imaginary parts were written separately with $z = x+iy$, and then recall that $\overline{z}/|z|^2 = 1/z$, where $\overline{z}$ is the complex conjugate of z.

[6] If we put $N = 0$ in Matsuoka's expansion (5), we retrieve, after some calculations and several approximations, the same result as Knessl and Coffey (7).

terms in Paris's expansion are quite complicated to compute. Third, explicit error bounds are not currently available.

A natural approach to construct an algorithm with the desired properties is to take a similar integral representation and perform numerical integration instead of developing an asymptotic expansion symbolically. The integral representations behind the previous asymptotic formulas do not appear to be convenient for this purpose, since they involve nonsmooth functions (periodic Bernoulli polynomials) or require a summation over several integrals. We therefore use integrals with exponentially decreasing kernels, as in the previous computational work by Ainsworth and Howell [2], but with the addition of saddle point analysis (which is necessary to handle large n) and a rigorous treatment of error bounds.

2. Integral representations

We obtain the following formulas in terms of elementary integrands that are rapidly decaying and analytic on the path of integration. Although restricted to $\mathrm{Re}(v) > \frac{1}{2}$, they permit computation on the whole (s, v) and (n, v) domains through application of the recurrence relations

$$\zeta(s,v) = \zeta(s,v+1) + \frac{1}{v^s}, \qquad \gamma_n(v) = \gamma_n(v+1) + \frac{\log^n v}{v}. \tag{8}$$

Theorem 1. *The Hurwitz zeta function $\zeta(s,v)$ and the generalized Stieltjes constants $\gamma_n(v)$ may be represented by the following integrals*

$$\zeta(s,v) = \frac{\pi}{2(s-1)} \int_{-\infty}^{+\infty} \frac{(v-\frac{1}{2} \pm ix)^{1-s}}{\cosh^2 \pi x}\, dx \tag{9}$$

$$= \frac{\pi}{2(s-1)} \int_{0}^{\infty} \frac{(v-\frac{1}{2} - ix)^{1-s} + (v-\frac{1}{2} + ix)^{1-s}}{\cosh^2 \pi x}\, dx \tag{10}$$

$$= \frac{\pi}{2(s-1)} \int_{0}^{\infty} \frac{\cos\left[(s-1)\arctan \frac{2x}{2v-1}\right]}{(v^2 - v + \frac{1}{4} + x^2)^{\frac{1}{2}(s-1)} \cosh^2 \pi x}\, dx \tag{11}$$

and

$$\gamma_n(v) = -\frac{\pi}{2(n+1)} \int_{-\infty}^{+\infty} \frac{\log^{n+1}(v-\frac{1}{2} \pm ix)}{\cosh^2 \pi x}\, dx \tag{12}$$

$$= -\frac{\pi}{2(n+1)} \int_{0}^{\infty} \frac{\log^{n+1}(v-\frac{1}{2} - ix) + \log^{n+1}(v-\frac{1}{2} + ix)}{\cosh^2 \pi x}\, dx \tag{13}$$

respectively. All formulas hold for complex v and s such that $\mathrm{Re}(v) > \frac{1}{2}$ and $s \neq 1$.[7]

In order to prove the above formulas, we will use the contour integration method.[8]

[7] In these formulas "$\pm$" signifies that either sign can be taken. Throughout this paper when several "$\pm$" or "$\mp$" are encountered in the same formula, it signifies that either the upper signs are used everywhere or the lower signs are used everywhere (but not the mix of them).

[8] Note that since many formulas with the kernels decaying exponentially fast were already obtained in the past by Legendre, Poisson, Binet, Malmsten, Jensen, Hermite, Lindelöf and many others (see e.g. a formula for the digamma function on p. 541 [5], or [4] or [22]), it is possible that formulas similar or equivalent to those we derive in this section might appear in earlier sources of which we are not aware. In particular, after the publication of the second draft version of this work, we learnt that a formula equivalent to our (11) appears in two books by Srivastava

Proof. Consider the following line integral taken along a contour C consisting of the interval $[-R,+R]$ on the real axis and a semicircle of the radius R in the upper half-plane, denoted C_R,

$$\oint_C \frac{(a-iz)^{1-s}}{\cosh^2\pi z}\,dz \;=\; \int_{-R}^{+R}\frac{(a-ix)^{1-s}}{\cosh^2\pi x}\,dx \;+\; \int_{C_R}\frac{(a-iz)^{1-s}}{\cosh^2\pi z}\,dz\,. \tag{14}$$

On the contour C_R the last integral may be bounded as follows:

$$\left|\int_{C_R}\frac{(a-iz)^{1-s}}{\cosh^2\pi z}\,dz\right| \;=\; R\left|\int_0^{\pi}\frac{(a-iRe^{i\varphi})^{1-s}e^{i\varphi}}{\cosh^2(\pi Re^{i\varphi})}\,d\varphi\right| \;\le$$

$$\le\; R\max_{\varphi\in[0,\pi]}\left|(a-iRe^{i\varphi})^{1-s}\right|\cdot I_R$$

$$\le\; R\max_{\varphi\in[0,\pi]}\Big[|a|^2+2R\,(a_x\sin\varphi-a_y\cos\varphi)+R^2\Big]^{\frac{1}{2}\,\mathrm{Re}\,(1-s)}e^{\pi|\mathrm{Im}(1-s)|}\,I_R \tag{15}$$

where we denoted $a_x\equiv\mathrm{Re}(a)$, $a_y\equiv\mathrm{Im}(a)$ and

$$I_R\;\equiv\;\int_0^{\pi}\frac{d\varphi}{|\cosh(\pi Re^{i\varphi})|^2}\,,\qquad R>0\,,$$

for the purpose of brevity. It can be shown that as R tends to infinity and remains integer the integral I_R tends to zero as $1/R$. For this aim, we first remark that

$$\frac{1}{|\cosh(\pi Re^{i\varphi})|^2}\;=\;\frac{2}{\cosh(2\pi R\cos\varphi)+\cos(2\pi R\sin\varphi)}\,.$$

Since R and φ are both real, $\cosh(2\pi R\cos\varphi)>1$ except for the case when $\cos\varphi=0$. Hence

$$\cosh(2\pi R\cos\varphi)+\cos(2\pi R\sin\varphi)>0\,,$$

except perhaps at $\varphi=\frac{1}{2}\pi$. But at the latter point, since R is integer,

$$\cosh(2\pi R\cos\varphi)+\cos(2\pi R\sin\varphi)\Big|_{\varphi=\frac{1}{2}\pi}\;=\;1+\cos(2\pi R)\;=\;2\,.$$

Therefore $|\cosh(\pi Re^{i\varphi})|^{-2}$ remains always bounded for integer R (see also Fig. 1), and when $R\to\infty$ we have

$$\frac{1}{|\cosh(\pi Re^{i\varphi})|^2}\;=\;\begin{cases}O(e^{-2\pi R\cos\varphi})\,, & \varphi\in[0,\frac{1}{2}\pi]\,,\\[2ex] O(e^{+2\pi R\cos\varphi})\,, & \varphi\in[\frac{1}{2}\pi,\pi]\,.\end{cases} \tag{16}$$

Thus, accounting for the symmetry of $|\cosh(\pi Re^{i\varphi})|^{-2}$ about $\varphi=\frac{1}{2}\pi$, we deduce that

$$\begin{aligned}I_R\;&=\int_0^{\pi}\frac{2\,d\varphi}{\cosh(2\pi R\cos\varphi)+\cos(2\pi R\sin\varphi)}\\ &=\int_0^{\frac{\pi}{2}}\frac{4\,d\varphi}{\cosh(2\pi R\cos\varphi)+\cos(2\pi R\sin\varphi)}\end{aligned}$$

and Choi, [28, p. 92, Eq. (23)] and [29, p. 160, Eq. (23)] respectively. In both sources it appears without proof and without references to other sources.

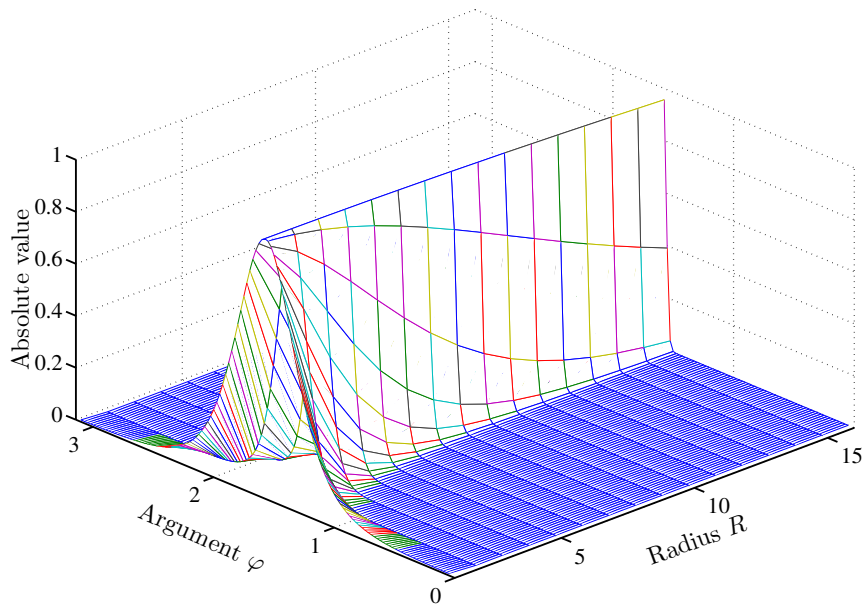

FIGURE 1. 3D-plot of $\left|\cosh\left(\pi R e^{i\varphi}\right)\right|^{-2}$ for $R \in [1, 16]$ and $\varphi \in [0, \pi]$ clearly displays the boundness of the latter (R integer). Note also that at large R the contribution of the point $\varphi = \frac{1}{2}\pi$ to the integral I_R becomes infinitely small (its height equals one, while the width tends to zero).

$$= O\left(\int_0^{\frac{\pi}{2}} e^{-2\pi R\cos\varphi}\, d\varphi\right) = O\left(\int_0^{\frac{\pi}{2}} e^{-2\pi R\sin\vartheta}\, d\vartheta\right), \qquad R \to \infty\,. \tag{17}$$

From the inequality

$$\frac{2\vartheta}{\pi} \le \sin\vartheta \le \vartheta\,, \qquad \vartheta \in [0, \tfrac{1}{2}\pi]\,,$$

it follows that

$$\frac{1 - e^{-\pi^2 R}}{2\pi R} \le \int_0^{\frac{\pi}{2}} e^{-2\pi R\sin\vartheta}\, d\vartheta \le \frac{1 - e^{-2\pi R}}{4R}\,, \tag{18}$$

and since R is large, exponential terms on both sides may be neglected. Thus $I_R = O(1/R)$ at $R \to \infty$.[9] Inserting this result into (15), we obtain

$$\left|\int_{C_R} \frac{(a - iz)^{1-s}}{\cosh^2 \pi z}\, dz\right| \to 0 \qquad \text{as} \quad R \to \infty\,,\, R \in \mathbb{N}\,, \tag{20}$$

[9]Another way to obtain the same result is to recall that the integral (18) may be evaluated in terms of the modified Bessel function $I_n(z)$ of the first kind and the modified Struve function $L_n(z)$. Using the asymptotic expansions of these special functions we obtain even a more exact result, namely

$$\int_0^{\frac{\pi}{2}} e^{-2\pi R\sin\vartheta}\, d\vartheta = \frac{\pi}{2}\Big\{I_0(2\pi R) - L_0(2\pi R)\Big\} \sim \frac{1}{2\pi R}\,, \qquad R \to \infty\,, \tag{19}$$

i.e. the integral asymptotically tends to the left bound (18).

if $\mathrm{Re}(s) > 1$. Hence, making $R \to \infty$, equality (14) becomes

$$\int_{-\infty}^{+\infty} \frac{(a-ix)^{1-s}}{\cosh^2 \pi x}\, dx \;=\; \oint_C \frac{(a-iz)^{1-s}}{\cosh^2 \pi z}\, dz \tag{21}$$

where the latter integral is taken around an infinitely large semicircle in the upper half-plane. The integrand is not a holomorphic function: it has the poles of the second order at $z = z_n \equiv i\left(n+\frac{1}{2}\right)$, $n \in \mathbb{N}_0$, due to the hyperbolic secant, and a branch point at $z = -ia$ due to the term in the numerator. If $\mathrm{Re}(a) > 0$, the branch point lies outside the integration contour and we may use the Cauchy residue theorem:

$$\oint_C \frac{(a-iz)^{1-s}}{\cosh^2 \pi z}\, dz \;=\; 2\pi i \sum_{n=0}^{\infty} \operatorname*{res}_{z=z_n} \frac{(a-iz)^{1-s}}{\cosh^2 \pi z} \;= \tag{22}$$

$$= -\frac{2i}{\pi} \sum_{n=0}^{\infty} \frac{\partial}{\partial z}(a-iz)^{1-s}\Big|_{z=i\left(n+\frac{1}{2}\right)} =$$

$$= \frac{2(s-1)}{\pi} \sum_{n=0}^{\infty} \left(a+\tfrac{1}{2}+n\right)^{-s} \;=\; \frac{2(s-1)}{\pi}\, \zeta(s, a+\tfrac{1}{2})\,.$$

Equating (21) with the last result yields

$$\zeta(s, a+\tfrac{1}{2}) \;=\; \frac{\pi}{2(s-1)} \int_{-\infty}^{+\infty} \frac{(a-ix)^{1-s}}{\cosh^2 \pi x}\, dx\,, \qquad \mathrm{Re}(a) > 0\,. \tag{23}$$

Splitting the interval of integration in two parts $(-\infty, 0]$ and $[0, +\infty]$ and recalling that

$$(a+ix)^s + (a-ix)^s \;=\; 2(a^2+x^2)^{\frac{s}{2}} \cos\!\left(s \arctan \frac{x}{a}\right) \tag{24}$$

the latter expression may also be written as

$$\zeta(s, a+\tfrac{1}{2}) \;=\; \frac{\pi}{2(s-1)} \int_0^{\infty} \frac{(a+ix)^{1-s} + (a-ix)^{1-s}}{\cosh^2 \pi x}\, dx \tag{25}$$

$$= \frac{\pi}{s-1} \int_0^{\infty} \frac{\cos\left[(s-1)\arctan \frac{x}{a}\right]}{(a^2+x^2)^{\frac{1}{2}(s-1)} \cosh^2 \pi x}\, dx\,, \qquad \mathrm{Re}(a) > 0\,. \tag{26}$$

Setting $a = v - \frac{1}{2}$ in our formulas for $\zeta(s, a+\frac{1}{2})$, we immediately retrieve our (9)–(11). From the principle of analytic continuation it also follows that above integral formulas are valid for all complex $s \neq 1$ and $\mathrm{Re}(a) > 0$ (because of the branch point which should not lie inside the integration contour). Note that at $v = 1$ our formulas (9)–(11) reduce to Jensen's formulas for the ζ function [5, Eqs. (88)].

Now, in order to get the corresponding formulas for the generalized Stieltjes constant $\gamma_n(v)$ we proceed as follows. The function $(s-1)\zeta(s, a+\frac{1}{2})$ is holomorphic on the entire complex s–plane, and hence, may be expanded into a Taylor series. The latter expansion about $s = 1$ reads

$$(s-1)\zeta(s, a+\tfrac{1}{2}) \;=\; 1 + \sum_{n=0}^{\infty} \frac{(-1)^n \gamma_n(a+\frac{1}{2})}{n!}\, (s-1)^{n+1}\,, \quad s \in \mathbb{C} \setminus \{1\}.$$

But $(s-1)\zeta(s, a+\frac{1}{2})$ also admits integral representations (23) and (25). Expanding them into the Taylor series in a neighborhood of $s = 1$ and equating coefficients in

$(s-1)^{n+1}$ produces formulas (12)–(13). As a particular case of these formulas we obtain formula (5) from [5] when $v=1$. □

Corollary 1. For complex v and s such that $\mathrm{Re}(v)>\frac{1}{2}$ and $s\neq 1$, the Hurwitz zeta function $\zeta(s,v)$ and the generalized Stieltjes constants $\gamma_n(v)$ admit the representations

$$\zeta(s,v) = \frac{(v-\frac{1}{2})^{1-s}}{s-1} + i\int_0^\infty \frac{(v-\frac{1}{2}-ix)^{-s}-(v-\frac{1}{2}+ix)^{-s}}{e^{2\pi x}+1}\,dx \tag{27}$$

$$= \frac{(v-\frac{1}{2})^{1-s}}{s-1} - 2\int_0^\infty \frac{\sin\left[s\arctan\frac{2x}{2v-1}\right]}{(v^2-v+\frac{1}{4}+x^2)^{\frac{s}{2}}}\cdot\frac{dx}{e^{2\pi x}+1} \tag{28}$$

and

$$\begin{aligned}\gamma_n(v) = &-\frac{\log^{n+1}(v-\frac{1}{2})}{n+1} + \\ &+ i\int_0^\infty \left\{\frac{\log^n(v-\frac{1}{2}-ix)}{v-\frac{1}{2}-ix} - \frac{\log^n(v-\frac{1}{2}+ix)}{v-\frac{1}{2}+ix}\right\}\frac{dx}{e^{2\pi x}+1}\end{aligned} \tag{29}$$

respectively.

Proof. Let $f(x)$ be such that $f(x)=o(e^{2\pi x})$ as $x\to\infty$. Then, by integration by parts one has

$$\int_0^\infty \frac{f(x)}{\cosh^2\pi x}\,dx = \frac{f(0)}{\pi} + \frac{2}{\pi}\int_0^\infty \frac{f'(x)}{e^{2\pi x}+1}\,dx\,, \tag{30}$$

provided the convergence of both integrals and the existence of $f(0)$. Putting $f(x)=(a+ix)^{1-s}+(a-ix)^{1-s}$ straightforwardly yields (27). By virtue of

$$(a+ix)^s-(a-ix)^s = 2i(a^2+x^2)^{\frac{s}{2}}\sin\left(s\arctan\frac{x}{a}\right), \tag{31}$$

we also obtain (28). We remark that at $v=1$ formulas (27)–(28) reduce to yet another formula of Jensen for the ζ function [5, Eqs. (88)] and its differentiated form. Formula (29) is obtained analogously from integral (13). □

Remark 1. For real $v>\frac{1}{2}$, our formulas for the Stieltjes constants may be simplified to

$$\gamma_n(v) = -\frac{\pi}{n+1}\,\mathrm{Re}\left\{\int_0^\infty \frac{\log^{n+1}(v-\frac{1}{2}\pm ix)}{\cosh^2\pi x}\,dx\right\} \tag{32}$$

and to

$$\gamma_n(v) = -\frac{\log^{n+1}(v-\frac{1}{2})}{n+1} \pm 2\,\mathrm{Im}\left\{\int_0^\infty \frac{\log^n(v-\frac{1}{2}\pm ix)}{v-\frac{1}{2}\pm ix}\cdot\frac{dx}{e^{2\pi x}+1}\right\} \tag{33}$$

respectively.

Remark 2. Using similar techniques one may obtain many other integral formulas with kernels decreasing exponentially fast, for instance:

$$\zeta(s) = \frac{1}{1-2^{s-1}}\left\{\frac{1}{2}+\frac{1}{2i}\int_{-\infty}^{+\infty}(1-ix)^{-s}\frac{dx}{\sinh\pi x}\right\} = \tag{34}$$

$$= \frac{1}{1-2^{s-1}}\left\{\frac{1}{2} + \int_0^\infty \frac{\sin\left(s\arctan x\right)}{(1+x^2)^{\frac{s}{2}}\sinh \pi x}\,dx\right\}, \tag{35}$$

$$\zeta(s,v) = \pm\frac{i\,\pi^2}{(s-1)(s-2)}\int_{-\infty}^{+\infty}(v-\tfrac{1}{2}\pm ix)^{2-s}\frac{\sinh\pi x}{\cosh^3\pi x}\,dx = \tag{36}$$

$$= \frac{2\,\pi^2}{(s-1)(s-2)}\int_0^\infty \frac{\sin\Big[(s-2)\arctan\frac{2x}{2v-1}\Big]}{(v^2-v+\frac{1}{4}+x^2)^{\frac{s}{2}-1}}\cdot\frac{\sinh\pi x}{\cosh^3\pi x}\,dx\,, \tag{37}$$

$$\zeta(s,v) = \frac{3\pi^3}{(s-1)(s-2)(s-3)}\int_{-\infty}^{+\infty}\left\{\frac{1}{\cosh^4\pi x} - \frac{2}{3\cosh^2\pi x}\right\}\frac{dx}{(v-\frac{1}{2}\pm ix)^{s-3}}\,, \tag{38}$$

$$\gamma_1 = \frac{\pi^2}{24} - \frac{\gamma^2}{2} - \frac{\log^2 2}{2} + \frac{\log^2\pi}{2} - \log 2\cdot\log\pi + \int_0^\infty \frac{\arctan x\cdot\log(1+x^2)}{\sinh\pi x}\,dx\,, \tag{39}$$

$$\gamma_n(v) = \frac{(-1)^{n+1}}{4\pi}\Big\{n(n-1)\zeta^{(n-2)}(3,v) + 3n\zeta^{(n-1)}(3,v) + 2\zeta^{(n-2)}(3,v)\Big\} -$$

$$-\frac{3\pi}{4(n+1)}\int_{-\infty}^{+\infty}\frac{\log^{n+1}(v-\frac{1}{2}\pm ix)}{\cosh^4\pi x}\,dx\,, \tag{40}$$

where the latter formulas hold for $\mathrm{Re}(v) > \frac{1}{2}$ and $n = 2,3,4,\ldots$ For the $n = 1$ case, one should remove the $n(n-1)\zeta^{(n-2)}(3,v)$ term from the last formula. The previous formulas for $\zeta(s,v)$ and $\gamma_n(v)$ also give rise to corresponding expressions for $\Psi(v)$ and $\log\Gamma(v)$. For example,

$$\Psi(v) = -\frac{\Psi_2(v)}{4\pi^2} + \frac{3\pi}{4}\int_0^\infty \frac{\log\left(v^2-v+\frac{1}{4}+x^2\right)}{\cosh^4\pi x}\,dx\,,$$

$$\log\Gamma(v) = \frac{1}{2}\log 2\pi + \left(v-\frac{1}{2}\right)\Big(\Psi(v)-1\Big) - \pi\int_0^\infty \frac{x\arctan\frac{2x}{2v-1}}{\cosh^2\pi x}\,dx\,,$$

$$\log\Gamma(v) = \frac{1}{2}\log 2\pi + \left(v-\frac{1}{2}\right)\left(\Psi(v) + \frac{\Psi_2(v)}{4\pi^2} - 1\right) -$$

$$-\frac{\Psi_1(v)}{4\pi^2} - \frac{3\pi}{2}\int_0^\infty \frac{x\arctan\frac{2x}{2v-1}}{\cosh^4\pi x}\,dx\,,$$

where $\Psi_1(v)$ and $\Psi_2(v)$ are the trigamma and tetragamma functions respectively.[10]

It is similarly possible to derive integral representations for the Lerch transcendent $\Phi(z,s,v) = \sum_{n=0}^\infty z^n(n+v)^{-s}$, for example

$$\Phi(z,s,v) = \frac{v^{-s}}{2} + \frac{i}{2}\int_0^\infty \frac{(-z)^{ix}(v+ix)^{-s} - (-z)^{-ix}(v-ix)^{-s}}{\sinh\pi x}\,dx$$

[10]Some other integral representations with the kernels decreasing exponentially fast for $\log\Gamma(v)$ and the polygamma functions may also be found in [4] and [5]. Also, various relationships between $\log\Gamma(z)$ and the polygamma functions are given and discussed in [4], [5] and [7].

$$= \frac{v^{-s}}{2} + \int_0^\infty \frac{\cos(x\log z)\sin\left[s\arctan\frac{x}{v}\right] - \sin(x\log z)\cos\left[s\arctan\frac{x}{v}\right]}{(v^2+x^2)^{\frac{s}{2}}\tanh\pi x}\,dx,$$

valid for $z > 0$, or

$$\begin{aligned}\zeta(s,v) &= \frac{v^{-s}}{2} + \frac{i}{2}\int_0^\infty \frac{e^{-\pi x}(v+ix)^{-s} - e^{+\pi x}(v-ix)^{-s}}{\sinh\pi x}\,dx \\ &= \frac{v^{-s}}{2} + \frac{i}{2}\int_0^\infty \frac{(v+ix)^{-s} - (v-ix)^{-s}}{\tanh\pi x}\,dx \\ &= \frac{v^{-s}}{2} + \int_0^\infty \frac{\sin\left[s\arctan\frac{x}{v}\right]}{(v^2+x^2)^{\frac{s}{2}}\tanh\pi x}\,dx\,,\end{aligned}$$

whose integrands are not of exponential decay, despite the presence of the hyperbolic cosecant.[11] At the same time, the above formula for $\Phi(z,s,v)$ is suitable for $z > 0$, while the same formula for the negative first argument reads

$$\Phi(-z,s,v) = \frac{v^{-s}}{2} + \frac{i}{2}\int_0^\infty \frac{z^{ix}(v+ix)^{-s} - z^{-ix}(v-ix)^{-s}}{\sinh\pi x}\,dx$$

$$= \frac{v^{-s}}{2} + \int_0^\infty \frac{\cos(x\log z)\sin\left[s\arctan\frac{x}{v}\right] - \sin(x\log z)\cos\left[s\arctan\frac{x}{v}\right]}{(v^2+x^2)^{\frac{s}{2}}\sinh\pi x}\,dx,$$

$z > 0$, and the integrand decreases exponentially fast.

3. Computation of $\gamma_n(v)$ by integration

For the computation of $\gamma_n(v)$, we use formulas (12)–(13), (32).[12] For the purpose of brevity throughout this section, we write a for $v - \frac{1}{2}$. We denote the integrand (with a and n as implicit parameters) and the half-line integral by

$$f(z) \equiv \frac{\log^{n+1}(a+iz)}{\cosh^2\pi z}\,, \qquad I_n(a) \equiv \int_0^\infty f(x)\,dx \tag{41}$$

respectively. After applying (8) as needed to ensure $\mathrm{Re}(a) > 0$ (or better, $\mathrm{Re}(a) \geq \frac{1}{2}$ to stay some distance away from the logarithmic branch point and avoid convergence issues during the numerical integration to follow), we may compute

$$\gamma_n(v) = -\frac{\pi}{(n+1)} \cdot \begin{cases} 2\,\mathrm{Re}(I_n(a)), & \mathrm{Im}(a) = 0 \\ I_n(a) + \overline{I_n(\overline{a})}, & \mathrm{Im}(a) \neq 0. \end{cases} \tag{42}$$

where "$\overline{}$" stands for the complex conjugate.

For a given accuracy goal of p bits, we aim to compute $I_n(a)$ with a relative error less than 2^{-p}. More precisely, we assume use of ball arithmetic [31], and we aim to compute an enclosure with relative radius less than 2^{-p}. A first important observation is that the computations must be done with a working precision of about $p + \log_2 n$ bits for p-bit accuracy, due to the sensitivity of the integrand. In other words, we lose about $\log_2 n$ bits to the exponents of the floating-point numbers

[11] Note that the second form of these expressions is obtained from the former one by a trivial simplification. Moreover, if we remark that $\coth\pi x = 1 + 2(e^{2\pi x} - 1)^{-1}$, we readily notice the relationship between these integrals and the Hermite and Jensen formulas for the ζ functions.

[12] Note that formulas (29), (33) can also provide good computational results.

when evaluating exponentials. Heuristically, a few more guard bits in addition to this will be sufficient to account for all rounding errors, and the computed ball provides a final certificate.

A technical point is that we cannot make any a priori statements about the relative error of $\gamma_n(v)$ since we do not have lower bounds for $|\gamma_n(v)|$. Cancellation is possible in the final addition (or extraction of the real part) in (42). This should roughly correspond to multiplying by the cosine factor in (7); it is reasonable to set the accuracy goal with respect to the nonoscillatory factor $Be^{nA}/\sqrt{n}$.

We primarily have in mind "small" parameters v (for example $v = 1$) such that $|v| \ll n$ if n is large. The algorithm works for any complex v where $\gamma_n(v)$ is defined, but we do not specifically address optimization for large $|v|$ which therefore may result in deteriorating efficiency and less precise output enclosures.

3.1. **Estimation of the tail.** We approximate $I_n(a)$, given by (41), by the truncated integral $\int_0^N f(x)\,dx$ for some $N > 0$. The following theorem provides an upper bound for the tail T_N.

Theorem 2. *Let*

$$T_N \equiv \int_N^\infty \frac{\log^{n+1}(a+ix)}{\cosh^2 \pi x}\,dx \tag{43}$$

and assume $\mathrm{Re}(a) > 0$. *Then, the following bound holds:*

$$|T_N| < 0.934\, e^{-2\pi N} |\log(a+Ni)|^{n+1}, \qquad N \geq n+2+|\mathrm{Im}(a)|\,. \tag{44}$$

Proof. For $x \geq 0$, using $|\log'(z)| = 1/|z|$ and the assumptions on a and N gives

$$\begin{aligned}
|\log(a+i(N+x))|^{n+1} &= |\log(a+Ni)|^{n+1} \left| 1 + \frac{\log(a+i(N+x)) - \log(a+Ni)}{\log(a+Ni)} \right|^{n+1} \\
&\leq |\log(a+Ni)|^{n+1} \left(1 + \frac{x}{|a+Ni|\,|\log(a+Ni)|} \right)^{n+1} \\
&\leq |\log(a+Ni)|^{n+1} \exp\left(\frac{(n+1)x}{|a+Ni| \log|a+Ni|} \right) \\
&\leq |\log(a+Ni)|^{n+1} \exp(2x).
\end{aligned}$$

Since $\mathrm{sech}^2(x) < 4e^{-2x}$ on the whole real line, we have

$$\begin{aligned}
|T_N| &\leq \int_N^\infty 4e^{-2\pi x} \left|\log(a+ix)\right|^{n+1} dx \\
&\leq 4e^{-2\pi N} |\log(a+Ni)|^{n+1} \int_0^\infty \exp\left(-2\pi x + 2x\right) dx
\end{aligned}$$

and the last integral equals $\frac{1}{2}(\pi - 1)^{-1}$. □

We can select N by starting with $N = n+2+|\mathrm{Im}(a)|$ and repeatedly doubling N until $|T_N| \leq 2^{-p-20}$, say. This bound does not need to be tight since the integration algorithm, described later, discards negligible segments cheaply through bisection.

Remark 3. The bound in the previous theorem can be made slightly sharper, although this does not matter for the algorithm. By using the same line of reasoning

as above, the inequality $|\log(1+z)| < \sqrt{|z|}$ holding true for $\mathrm{Re}(z) \geq 0$ and the fact that the error function is always lesser than 1, one can obtain, for example,

$$|T_N| < 0.637\Big(1 + \tfrac{\lambda}{\sqrt{2}}\, e^{\frac{\lambda^2}{8\pi}}\Big) e^{-2\pi N} |\log(a+Ni)|^{n+1}\,, \qquad N \geq \frac{4(n+1)^2}{\lambda^2} + |\mathrm{Im}(a)|\,,$$

where λ is some positive parameter lesser than 2 (the smaller λ, the better this estimation; for $\lambda < 0.649$ this estimation outperforms (44), but N must be large with respect to n^2). Moreover, for $0 < \lambda \ll 1$ we may neglect the term $O(\lambda)$ between the parenthesis, and hence obtain

$$|T_N| \lessapprox 0.637\, e^{-2\pi N} |\log(a+Ni)|^{n+1}, \quad N \gg n^2\,.$$

Both these bounds and the value 0.637, coming from $2/\pi$, are in good agreement with the numerical results. Note that if (44) is suitable for cases in which N is comparable to n, the above estimations are suitable only for cases of large and extra-large N with respect to n^2.

3.2. **Cancellation-avoiding contour.** For small n, the integral $\int_0^N f(x)\,dx$ can be computed directly. For large n, the integrand oscillates on the real line and a higher working precision must be used due to cancellation. At least for $v = 1$, the amount of cancellation can be calculated accurately by numerically computing the maximum value of $|f(x)|$ on $0 \leq x < \infty$ and comparing this magnitude to the asymptotic formula (7). For example, we need about 30 extra bits when $n = 10^3$, 1740 bits when $n = 10^6$, and $4 \cdot 10^5$ bits when $n = 10^9$.

For n larger than about 10^3, we shift the path to eliminate the cancellation problem. The integrand can be written as

$$f(z) = \exp\left(g(z)\right) h(z), \tag{45}$$

where

$$g(z) = (n+1)\log\left(\log\left(a+iz\right)\right) - 2\pi z, \quad h(z) = (1+\tanh \pi z)^2. \tag{46}$$

Assuming that $n \gg |a|$, the function $\exp(g(z))$ has a single saddle point in the right half-plane. The saddle point equation $g'(\omega) = 0$ can be reduced to

$$(n+1) + 2\pi i\,(a+i\omega)\log\left(a+i\omega\right) = 0 \tag{47}$$

which admits the closed-form solution

$$\omega = i\left(a - \frac{u}{W_0(u)}\right), \quad u = \frac{(n+1)i}{2\pi}. \tag{48}$$

where $W_0(u)$ is the principal branch of the Lambert W function. Only the principal branch works, a fact which is not obvious from the symbolic form of the solution but which can be checked numerically.

We can now integrate along four segments

$$\int_0^N f(x)\,dx \;=\; \int_0^M f(z)\,dz + \int_M^{M+Ci} f(z)\,dz + \int_{M+Ci}^{N+Ci} f(z)\,dz + \int_{N+Ci}^{N} f(z)\,dz$$

with the choice of vertical offset $C = \mathrm{Im}(\omega)$ to (approximately) minimize the peak magnitude of $f(t+Ci)$ on $M \leq t \leq N$. The left point $M > 0$ just serves to avoid the poles of the integrand on the imaginary axis and the nearby vertical branch cut of the logarithm; we can for instance take $M = 10$.

Numerical tests (compare Fig. 2) confirm that there is virtually no cancellation with this contour (again, assuming that $|v|$ is not too large). The path does not

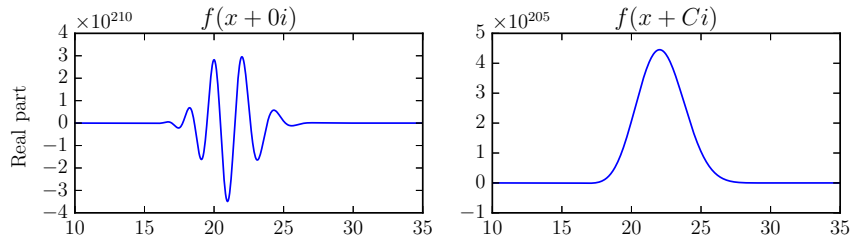

FIGURE 2. Real part of $f(z)$ for $z = x + 0i$ on the real line (left) and for $z = x + Ci$ passing near the saddle point (right), here with parameters $a = \frac{1}{2}, n = 500$, where integrating along the real line results in about five digits of cancellation.

exactly pass through the saddle point of $f(z)$, but since $h(z)$ is exponentially close to a constant, the perturbation is negligible. The deviation between the straight-line path through the saddle point and the actual steepest descent contour also has negligible impact on the numerical stability.

We note that the complex Lambert W function can be computed with rigorous error bounds [15]. However, it is not actually necessary to compute ω rigorously for this application since the integration follows a connected path and ball arithmetic will account for the actual cancellation; it is sufficient to use a floating-point approximation for ω with heuristic accuracy of about $\log_2 n$ bits. For example, an approximation of ω computed with 53-bit machine arithmetic is sufficient up to about $n = 10^{15}$.

3.3. **Integration and bounds near the saddle point.** The main task of integrating $f(z)$ along one or four segments in the plane is not difficult in principle, since $f(z)$ is analytic (and non-oscillatory) in a neighborhood of each segment. Constructing a reliable and fast algorithm, in particular for extremely large n, does nevertheless require some attention to detail.

Gauss-Legendre quadrature is a good option, and was already used by Ainsworth and Howell [2], who, however, did not prove any error bounds since "The integrand is much too complex to use the standard remainder terms". To obtain rigorous error bounds and ensure rapid convergence with a manageable level of manual error analysis, we use the self-validating Petras algorithm [26] which was recently adapted for arbitrary-precision ball arithmetic and implemented in the Arb library [17].

The Petras algorithm combines Gauss-Legendre quadrature with adaptive bisection. Given a segment $[\alpha, \beta]$, the algorithm first evaluates the direct enclosure $(\beta - \alpha) f([\alpha, \beta])$ and uses this if the error is negligible (which in this application always occurs near the tail ends of the integral when $p \ll n$). Otherwise, it bounds the error of d-point quadrature

$$\int_\alpha^\beta f(z)dz \approx \sum_{k=1}^{d} w_k f(z_k)$$

in terms of the magnitude $|f(z)|$ on a Bernstein ellipse E around $[\alpha, \beta]$: if $f(z)$ is analytic on E with $\max_{z \in E} |f(z)| \leq V$, the error is bounded by Vc/ρ^d where c and ρ only depend on E and $[\alpha, \beta]$. If $f(z)$ has poles or branch cuts on E or if the quadrature degree d determined by this bound would have to be larger than $O(p)$

to ensure a relative error smaller than 2^{-p}, the segment $[\alpha, \beta]$ is bisected and the same procedure is applied recursively.

The remaining issue is the evaluation of the integrand. The pointwise evaluations $w_k f(z_k)$ pose no problem: here we simply use (41) directly. It is slightly more complicated to compute good enclosures for $f(z)$ on wide intervals representing z, which is needed both for the direct enclosures on subintervals $f([\alpha, \beta])$ and for the bounds on ellipses.[13] Bounding the integrand on wide ellipses (or enclosing rectangles) by evaluating (41) or (45)–(46) directly in interval or ball arithmetic results at best in $n^{1/2+o(1)}$ complexity as $n \to \infty$.[14] The explanation for this phenomenon is that $f(z)$ is a quotient of two functions $f_1(z) = \log^{n+1}(a + iz)$, $f_2(z) = \cosh^2 \pi z$ that individually vary rapidly near the saddle point, i.e.

$$\frac{f_1(z+\varepsilon)}{f_1(z)} \sim \frac{f_2(z+\varepsilon)}{f_2(z)} \sim e^{2\pi\varepsilon} \tag{49}$$

while f_1/f_2 is nearly constant. Direct evaluation fails to account for this correlation, which is an example of the dependency problem in interval arithmetic. Therefore, although $f(z)$ is nearly constant close to the saddle point, direct upper bounds for $|f(z)|$ are exponentially sensitive to the width of input intervals, and this forces the integration algorithm to bisect down to subsegments of width $O(1)$ around the saddle point. Since the Gaussian peak of the integrand around the saddle point has an effective width of $O(n^{1/2})$, the integration algorithm has to bisect down to $O(n^{1/2})$ subsegments before converging.

To solve this problem, we compute tighter bounds on wide intervals using the standard trick of Taylor expanding with respect to a symbolic perturbation ε.

Theorem 3. *If z is contained in a disk or rectangle Z with midpoint m and radius r, such that* $\operatorname{Re}(Z) \geq 1$, *and if* $\max_{|u-m|\leq r} |g''(u)| \leq G$, *then*

$$|f(z)| < 4.015\, |\exp(g(m))| \exp\left(|g'(m)| r + \tfrac{1}{2} G r^2\right). \tag{50}$$

Proof. We use the decomposition (45)–(46). If $\operatorname{Re}(z) \geq 1$, then $|h(z)| < 4.015$. Taylor's theorem applied to $\exp(g(z))$ gives

$$\exp(g(m+\varepsilon)) = \exp(g(m)) \exp\left(g'(m)\varepsilon + \int_0^\varepsilon g''(m+t)(\varepsilon - t)\,dt\right) \tag{51}$$

for all $|\varepsilon| \leq r$. □

To implement the bound (50), we compute $g(m)$ and $g'(m)$ in ball arithmetic (where m is an exact floating-point number), using the formula

$$g'(m) = \frac{i(n+1)}{(a+im)\log(a+im)} - 2\pi.$$

The behavior near the saddle point is now captured precisely by the cancellation in $g'(m)$. At least $\log_2 n$ bits of precision must be used to evaluate $\exp(g(m))$ (to ensure that the magnitude of the integrand near the peak is approximated accurately)

[13] The complex ball arithmetic in Arb actually uses rectangles with midpoint-radius real and imaginary parts rather than complex disks, so ellipses will always be represented by enclosing rectangles (with up to a factor $\sqrt{2}$ overestimation), but this detail is immaterial to the principle of the algorithm.

[14] In fact, the complexity becomes $n^{1+o(1)}$ when using ball arithmetic with a fixed precision for the radii (30 bits in Arb). The $n^{1/2+o(1)}$ estimate holds when the endpoints are tracked accurately.

and also to evaluate $g'(m)$ (to ensure that the remainder after the catastrophic cancellation is evaluated accurately). Finally, to compute G, we evaluate

$$g''(z) = \frac{(n+1)\left(1+\frac{1}{\log t}\right)}{t^2 \log t}, \quad t = a + iz$$

directly over the complex ball representing z. As a minor optimization, we can compute lower bounds for $|t|$ and $|\log t|$. This completes the algorithm.

3.4. **Asymptotic complexity.** If the accuracy goal p is fixed (or grows sufficiently slowly compared to n), then we can argue heuristically that the bit complexity of computing γ_n to p-bit accuracy with this algorithm is $\log^{2+o(1)} n$. This estimate accounts for the bisection depth around the saddle point as well as the extra precision of $\log_2 n$ bits. The logarithmic complexity agrees well with the actual timings (presented in the next section).

We stop short of attempting to prove a formal complexity result, which would require more detailed calculations and careful accounting for the accuracy of the enclosures in ball arithmetic as well as details about the integration algorithm. We have delegated as much work as possible to a general-purpose integration algorithm in order to minimize the analysis necessary for a complete implementation. However, in future work, it would be interesting to pursue such analysis not just for this specific problem, but more generally for evaluating classes of parametric integrals using the combination of saddle point analysis and numerical integration.

If we on the other hand fix n and consider varying p, then the asymptotic bit complexity is of course $p^{2+o(1)}$ since Gaussian quadrature uses $O(p)$ evaluations of the integrand on a fixed segment and $O(\log p)$ segments are sufficient.

4. Implementation and benchmark results

The new integration algorithm has been implemented in Arb [14].[15] The method `acb_dirichlet_stieltjes` computes $\gamma_n(v)$, given a complex ball representing v, an arbitrary-size integer n, and a precision p. The working precision is set automatically so that the result will be accurate to about p bits, at least when $v = 1$. This method selects automatically between two internal methods:

- `acb_dirichlet_stieltjes_integral` uses the new integration algorithm.
- `acb_dirichlet_stieltjes_em` is a wrapper around the existing code for computing the Hurwitz zeta function using Euler-Maclaurin summation [13].

For very small n, the integration algorithm is one–three orders of magnitude slower than Euler-Maclaurin summation, but the cost of the latter increases rapidly with n. Integration was found to be faster when $n > \max(100, p/2)$, and this automatic cutoff is used in the code. We remark that the Euler-Maclaurin code actually computes $\gamma_0(v), \ldots, \gamma_n(v)$ simultaneously and reads off the last entry. At this time, we do not have an implementation of the Euler-Maclaurin formula optimized for a single $\gamma_n(v)$ value, which would be significantly faster for n from about 10 to 10^3.

Table 1 shows the time in seconds to evaluate the ordinary Stieltjes constants γ_n to a target accuracy p of 64 bits (about 18 digits), 333 bits (about 100 digits) and 3333 bits (just more than 1000 digits) on an Intel Core i5-4300U CPU running 64-bit Ubuntu Linux. Here we only show the timing results for the Arb method `acb_dirichlet_stieltjes_integral`, omitting use of Euler-Maclaurin summation.

[15] `http://arblib.org/` – the new code is available in the 2.14-git version.

TABLE 1. Time in seconds to compute γ_n. The left columns show results for d digits in Mathematica using `N[StieltjesGamma[n],d]`, or `N[StieltjesGamma[n]]` when $d = 16$ giving machine precision. The smallest results are omitted since the timer in Mathematica does not have sufficient resolution. The (wrong) entries signify that Mathematica returns an incorrect result. The (timeout) entries signify that Mathematica had not completed after several hours. The right columns show results for p-bit precision with the new integration algorithm in Arb.

	Mathematica			Arb (integration)		
n	$d = 16$	$d = 100$	$d = 1000$	$p = 64$	$p = 333$	$p = 3333$
1			0.16	0.0011	0.0089	2.7
10		0.016	0.39	0.0020	0.032	6.6
10^2	0.016	0.16	2.7	0.0032	0.030	3.5
10^3	0.031	0.16	3.3	0.0064	0.10	7.5
10^4	(wrong)	0.41	4.5	0.0043	0.045	19.8
10^5	(wrong)	(timeout)	(timeout)	0.0043	0.026	27.8
10^6	(wrong)			0.0066	0.026	18.1
10^{10}				0.0087	0.031	32.6
10^{15}				0.014	0.061	7.0
10^{30}				0.087	0.22	16.7
10^{60}				0.26	0.86	30.9
10^{100}				0.76	1.5	57.2

TABLE 2. Time in seconds to compute $\gamma_0, \ldots, \gamma_n$ simultaneously.

	Arb (Euler-Maclaurin)			Arb (integration)		
n	$p = 64$	$p = 333$	$p = 3333$	$p = 64$	$p = 333$	$p = 3333$
1	0.000061	0.00026	0.012	0.012	0.12	18
10	0.00035	0.0016	0.060	0.025	0.20	37
10^2	0.0047	0.11	0.39	0.28	1.8	370
10^3	0.69	0.87	5.5	4.3	23	4527
10^4	1207	1210	1626	38	267	

The table also shows timings for Mathematica 11.0.0 for Microsoft Windows (64-bit) on an Intel Core i9-7900X CPU for comparison.

As expected, the running time of our algorithm only depends weakly on n. The performance is also reasonable for large p. The timings fluctuate slightly rather than increasing monotonically with n, which appears to be an artifact of the local adaptivity of the integration algorithm.

Mathematica returns incorrect answers for large n when using machine precision. At higher precision, the performance is consistent up to about $n = 10^4$, but the running time then starts to increase rapidly. With $n = 10^5$ and 100-digit or 1000-digit precision, Mathematica did not finish when left to run overnight.

Mathematica uses Keiper's algorithm according to the documentation [30], but unfortunately we do not have details about the implementation. The timings and failures for large n are seemingly consistent with use of numerical integration in some form without the precautions we have taken against oscillation problems.

We also mention that Maple is much slower than Mathematica, taking 0.1 seconds to compute γ_{10}, a minute to compute γ_{1000} and six minutes to compute γ_{2000} to 10 digits.

4.1. **Multi-evaluation.** Table 2 compares the performance of Euler-Maclaurin summation and the integration method in Arb for computing $\gamma_0(v), \ldots, \gamma_n(v)$ simultaneously. With the integration algorithm, this means making $n+1$ independent evaluations, while the Euler-Maclaurin algorithm only has to be executed once. Despite this, integration still wins for sufficiently large n, unless p also is large.

4.2. **Numerical values.** We show the computed values of a few large Stieltjes constants. The following significands are correctly rounded to 100 digits (with at most 0.5 ulp error):

$$\gamma_{10^5} \approx 1.99192730631254109565822724315685892052116597775331132587597552593617125927222717691432066619096522 5 \cdot 10^{83432},$$

$$\gamma_{10^{10}} \approx 7.58836212371310519482240337991254869217504103245097004705409333849242397478392791499204665451855077 9 \cdot 10^{12397849705},$$

$$\gamma_{10^{15}} \approx 1.84410172558473229070326955983513648856757465533155879218608594850254260862772177902307157373202222 1 \cdot 10^{1452992510427658},$$

$$\gamma_{10^{100}} \approx 3.18743141870239927999741646992711665139430991088384692250710626598304893415593755966828802263230609 5 \cdot 10^{e},$$

$$e = 2346394292277254080949367838399091160903447689869837385205779111579215664052158234417125417543348369 4.$$

As a sanity check, γ_{10^5} agrees with the previous record Euler-Maclaurin computation [13]. The value of γ_n also agrees with the Knessl-Coffey formula (7) to about $\log_{10} n$ digits, in perfect agreement with the error term in this asymptotic approximation being $O(1/n)$.

For $\gamma_n(v)$ with a nonreal v, the computation time roughly doubles since two integrals are computed. With $v \neq 1$, we can for instance compute:

$$\gamma_{10^5}(2+3i) \approx (1.52933142489317896667092453331813941673604063614322663904691747102612382202869541466989081808995810 4 + 7.62660531702353922882984645453420273501336816533023070075187095010490600079192738743855497923063058i) \cdot 10^{83440},$$

$$\gamma_{10^{100}}(2+3i) \approx (0.02447197253567132691871635713584630519276677767177878733142765829147799303241971747565188937402242864 + 1.32811448545861696707866231220831954057981697325317951175064293043735977753817673157831879994069288 3i) \cdot 10^{e+10}.$$

These values similarly agree to $\log_{10} n$ digits with the leading-order truncation of Paris's generalization [25] of the Knessl-Coffey formula, providing both a check on our implementation and an independent validation of Paris's results.

5. Discussion

A few possible optimizations of the integration algorithm are worth pointing out. The adaptive integration strategy in Arb can probably be improved, which should give a constant factor speedup. The working precision could also likely be reduced by a preliminary rescaling near the saddle point.

For evaluating a range of $\gamma_n(v)$ simultaneously, one could perform vector-valued integration and recycle the evaluations of $\log(a+iz)$ and $\cosh^2 \pi z$. It would be interesting to compare this approach to simultaneous evaluation with the Euler-Maclaurin formula.

It would also be interesting to investigate use of double exponential quadrature instead of Gaussian quadrature.

The computational part of this study was done for two purposes: first, to develop working code for Stieltjes constants as part of the collection of rigorous special function routines in the Arb library, and second, to test the integration algorithm [26, 17] for a family of integrals involving large parameters. We do not have a concrete application in mind for the code, but the Stieltjes constants are potentially useful in various types of analytic computations involving the Riemann zeta function, and large-n evaluation can be useful for testing the accuracy of asymptotic formulas for Stieltjes constants and related quantities.

The technique of evaluating parametric integrals by integrating numerically along a steepest descent contour is, of course, well established in the literature on computational methods for special functions, but such an algorithm has not previously been published for Stieltjes constants. The use of rigorous integration techniques in such a setting has also been explored very little in earlier work. The most important lesson learned here is that the heavy lifting can be done by the integration algorithm, requiring only an elementary pen-and-paper analysis of the integrand. The same technique should be effective for rigorously computing many other number sequences and special functions given by similar integral representations. On that note, it would be interesting to search for more integral representations similar to those obtained in Section 2. Many such representations with the integrands decreasing exponentially fast for $\log \Gamma(z)$ and for the polygamma functions may be found in [4] and [5].

Acknowledgements

We thank Jacques Gélinas for pointing out the previous computations in [2] and Vladimir Reshetnikov for helping with some numerical verifications, and are especially greateful to Joseph Oesterlé for sharing many challenging ideas on the Stieltjes constants during his stay in St. Petersburg in June 2017.

References

[1] J. Adell and A. Lekuona. Fast computation of the Stieltjes constants. *Mathematics of Computation*, 86(307):2479–2492, 2017.

[2] O. R. Ainsworth and L. W. Howell. An integral representation of the generalized Euler-Mascheroni constants. *NASA Technical Paper 2456*, 1985.

[3] B. C. Berndt. On the Hurwitz zeta-function. *The Rocky Mountain Journal of Mathematics*, 2(1):151–157, 1972.

[4] Ia. V. Blagouchine. Rediscovery of Malmsten's integrals, their evaluation by contour integration methods and some related results. *Ramanujan Journal*, 35:21–110, 2014. Addendum: 42:777–781, 2017.

[5] Ia. V. Blagouchine. A theorem for the closed-form evaluation of the first generalized Stieltjes constant at rational arguments and some related summations. *Journal of Number Theory*, 148:537–592, 2015. Erratum: 151:276–277, 2015.

[6] Ia. V. Blagouchine. Expansions of generalized Euler's constants into the series of polynomials in π^{-2} and into the formal enveloping series with rational coefficients only. *Journal of Number Theory*, 158:365–396, 2016. Corrigendum: 173:631–632, 2017.

[7] Ia. V. Blagouchine. Three notes on Ser's and Hasse's representations for the zeta-functions. *Integers*, 18A(#A3):1–45, 2018.
[8] J. Bohman and C. E. Fröberg. The Stieltjes function - definition and properties. *Mathematics of Computation*, 51(183):281–289, 1988.
[9] R. P. Brent and E. M. McMillan. Some new algorithms for high-precision computation of Euler's constant. *Mathematics of Computation*, 34(149):305–312, 1980.
[10] W. E. Briggs. Some constants associated with the Riemann zeta-function. *The Michigan Mathematical Journal*, 3(2):117–121, 1955.
[11] L. Fekih-Ahmed. A new effective asymptotic formula for the Stieltjes constants. *arXiv preprint arXiv:1407.5567*, 2014.
[12] J. P. Gram. Note sur le calcul de la fonction $\zeta(s)$ de Riemann *Oversigt. K. Danske Vidensk. (Selsk. Forh.)*, 303–308, 1895.
[13] F. Johansson. Rigorous high-precision computation of the Hurwitz zeta function and its derivatives. *Numerical Algorithms*, 69:253–270, 2015.
[14] F. Johansson. Arb: efficient arbitrary-precision midpoint-radius interval arithmetic. *IEEE Transactions on Computers*, 66:1281–1292, 2017.
[15] F. Johansson. Computing the Lambert W function in arbitrary-precision complex interval arithmetic. *arXiv preprint arXiv:1705.03266*, 2017.
[16] F. Johansson. mpmath: a Python library for arbitrary-precision floating-point arithmetic, 2017. Version 1.0.
[17] F. Johansson. Numerical integration in arbitrary-precision ball arithmetic. *arXiv preprint arXiv:1802.07942*, 2018.
[18] J. B. Keiper. Power series expansions of Riemann's ξ function. *Mathematics of Computation*, 58(198):765–773, 1992.
[19] C. Knessl and M. Coffey. An effective asymptotic formula for the Stieltjes constants. *Mathematics of Computation*, 80(273):379–386, 2011.
[20] R. Kreminski. Newton-Cotes integration for approximating Stieltjes (generalized Euler) constants. *Mathematics of Computation*, 72(243):1379–1397, 2003.
[21] J. J. Y. Liang and J. Todd. The Stieltjes constants. *Journal of Research of the National Bureau of Standards*, 76:161–178, 1972.
[22] E. Lindelöf. Le calcul des résidus et ses applications à la théorie des fonctions. Gauthier–Villars, 1905.
[23] Y. Matsuoka. Generalized Euler constants associated with the Riemann zeta function. In "Number Theory and Combinatorics: Japan 1984 (Jin Akiyama ed.)". World Scientific, Singapore, 279–295, 1985.
[24] Y. Matsuoka. On the power series coefficients of the Riemann zeta function. *Tokyo Journal of Mathematics*, 12(1):49–58, 1989.
[25] R. B. Paris. An asymptotic expansion for the Stieltjes constants. *arXiv preprint arXiv:1508.03948*, 2015.
[26] K. Petras. Self-validating integration and approximation of piecewise analytic functions. *Journal of Computational and Applied Mathematics*, 145(2):345–359, 2002.
[27] S. Saad-Eddin. On two problems concerning the Laurent–Stieltjes coefficients of Dirichlet L–series (Ph.D. thesis). University Lille 1, France, 2013.
[28] H. M. Srivastava and J. Choi. Series Associated with the Zeta and Related Functions. Kluwer Academic Publishers, the Netherlands, 2001.
[29] H. M. Srivastava and J. Choi. Zeta and q–Zeta Functions and Associated Series and Integrals. Elsevier, 2012.
[30] Wolfram Research. Some notes on internal implementation. Wolfram Language & System Documentation Center, 2018. `https://reference.wolfram.com/language/tutorial/SomeNotesOnInternalImplementation.html`.
[31] J. van der Hoeven. Ball arithmetic. Technical report, HAL, 2009. hal-00432152.

LFANT – INRIA – IMB, Bordeaux, France
E-mail address: `fredrik.johansson@gmail.com`

SeaTech, University of Toulon, France
E-mail address: `iaroslav.blagouchine@univ-tln.fr`